

Synthesis, Structure, and Properties of $\text{Li}_2\text{In}_2\text{MQ}_6$ ($M = \text{Si}, \text{Ge}; Q = \text{S}, \text{Se}$): A New Series of IR Nonlinear Optical Materials

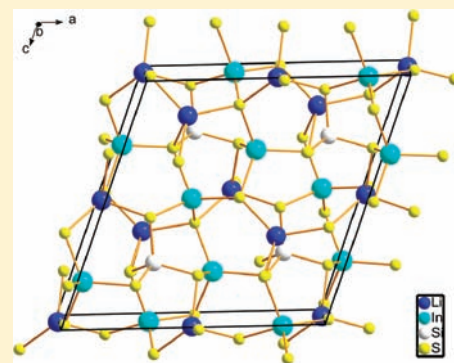
Wenlong Yin,^{†,‡,§} Kai Feng,^{†,‡,§} Wenyu Hao,^{†,‡,§} Jiyong Yao,^{*,†,‡} and Yicheng Wu^{†,‡}

[†]Center for Crystal Research and Development and [‡]Key Laboratory of Functional Crystals and Laser Technology, Technical Institute of Physics and Chemistry, Chinese Academy of Sciences, Beijing 100190, People's Republic of China

[§]Graduate University of the Chinese Academy of Sciences, Beijing 100049, People's Republic of China

Supporting Information

ABSTRACT: The four isostructural compounds $\text{Li}_2\text{In}_2\text{MQ}_6$ ($M = \text{Si}, \text{Ge}; Q = \text{S}, \text{Se}$) have been synthesized for the first time. They crystallize in the noncentrosymmetric monoclinic space group Cc with the three-dimensional framework composed of corner-sharing LiQ_4 , InQ_4 , and MQ_4 tetrahedra. The second-harmonic-generation signal intensities of the two sulfides and two selenides were close to those of AgGaS_2 and AgGaSe_2 , respectively, when probed with a laser with 2090 nm as the fundamental wavelength. They possess large band gaps of 3.61(2) eV for $\text{Li}_2\text{In}_2\text{SiS}_6$, 3.45(2) eV for $\text{Li}_2\text{In}_2\text{GeS}_6$, 2.54(2) eV for $\text{Li}_2\text{In}_2\text{SiSe}_6$, and 2.30(2) eV for $\text{Li}_2\text{In}_2\text{GeSe}_6$, respectively. Moreover, these four compounds all melt congruently at relatively low temperatures, which makes it feasible to grow bulk crystals needed for practical application by the Bridgman–Stockbarger method.



INTRODUCTION

Nowadays, frequency conversion through mid and far IR nonlinear optical (NLO) crystals is an important way to generate mid and far IR laser sources, which have many important civil and military applications including atmospheric monitoring, laser radar, and laser guidance. As a result of their large NLO coefficient and wide transparent range in the IR range, the chalcopyrite-type AgGaQ_2 ($Q = \text{S}, \text{Se}$)^{1,2} and ZnGeP_2 ³ crystals have been the practically used IR NLO materials since the 1970s. However, they possess serious drawbacks of one or another in their properties. For example, AgGaQ_2 ($Q = \text{S}, \text{Se}$) has a low laser-damage threshold, AgGaSe_2 is not phase-matchable at 1 μm , and ZnGeP_2 exhibits strong two-photon absorption of the conventional 1 μm (Nd:YAG) or 1.55 μm (Yb:YAG) laser-pumping sources.⁴ Thus, the search for new IR NLO materials with better overall properties has been very active in recent years.^{5–17}

Among all of the requirements for a good IR NLO material, increasing the laser-damage threshold and avoiding the two-photon absorption problem of the conventional near-IR laser-pumping sources are probably the two most demanding ones. An effective way of achieving these goals is to enlarge the band gap of the IR NLO material. The inclusion of alkali or alkaline-earth metals in synthesizing new IR NLO materials is conducive to increasing the band gaps of compounds. Thus, recently, extensive research has focused on alkali- or alkaline-earth metals containing chalcogenides with a high content of microscopic NLO-active units,^{5–12} such as GaQ_4 tetrahedra.^{18,19} The inclusion of an alkali or alkaline-earth metal will increase the band gap, and a dense arrangement of the microscopic NLO-active units will increase the possibility of

achieving a large macroscopic NLO response if they are aligned in a cooperative manner. In this way, compounds with a strong NLO response and large band gap could be obtained.

Besides optical properties, the easiness of obtaining bulk crystals is another important factor that influences the potential for practical application for IR NLO materials because bulk crystals are needed for the thorough evaluation and practical application of IR NLO materials. Nowadays, almost all bulk crystals of chalcogenides are grown by the Bridgman–Stockbarger method in sealed ampules, which indicates that the material needs to exhibit congruent-melting behavior. Thus, compounds exhibiting large NLO response, large band gaps, and congruent-melting behavior are of great importance because of their potential for practical application. Recently, we reported our discovery of the low-melting-point, low-lithium-content, new IR NLO material $\text{LiGaGe}_2\text{Se}_6$ in the $\text{Li}/\text{Ga}/\text{Ge}/\text{Q}$ ($Q = \text{S}, \text{Se}, \text{Te}$) system, which exhibits a second-harmonic-generation (SHG) response at 2 μm that is approximately half that of the benchmark material AgGaSe_2 and melts congruently at the rather low temperature of 710 °C. Detailed investigations on the growth technique and thorough evaluation of these crystals are in process.

In $\text{LiGaGe}_2\text{Se}_6$, the microscopic NLO-active unit is the $(\text{Ga}/\text{Ge})\text{Se}_4$ tetrahedron. Considering that the heavier group III element, In, will increase the NLO response and birefractive index owing to the larger polarization of the electrons, we extend our exploration to the $\text{Li}/\text{In}/\text{M}/\text{Q}$ ($M = \text{Si}, \text{Ge}; Q = \text{S}, \text{Se}, \text{Te}$) system and successfully obtained another new series of

Received: February 19, 2012

Published: May 4, 2012

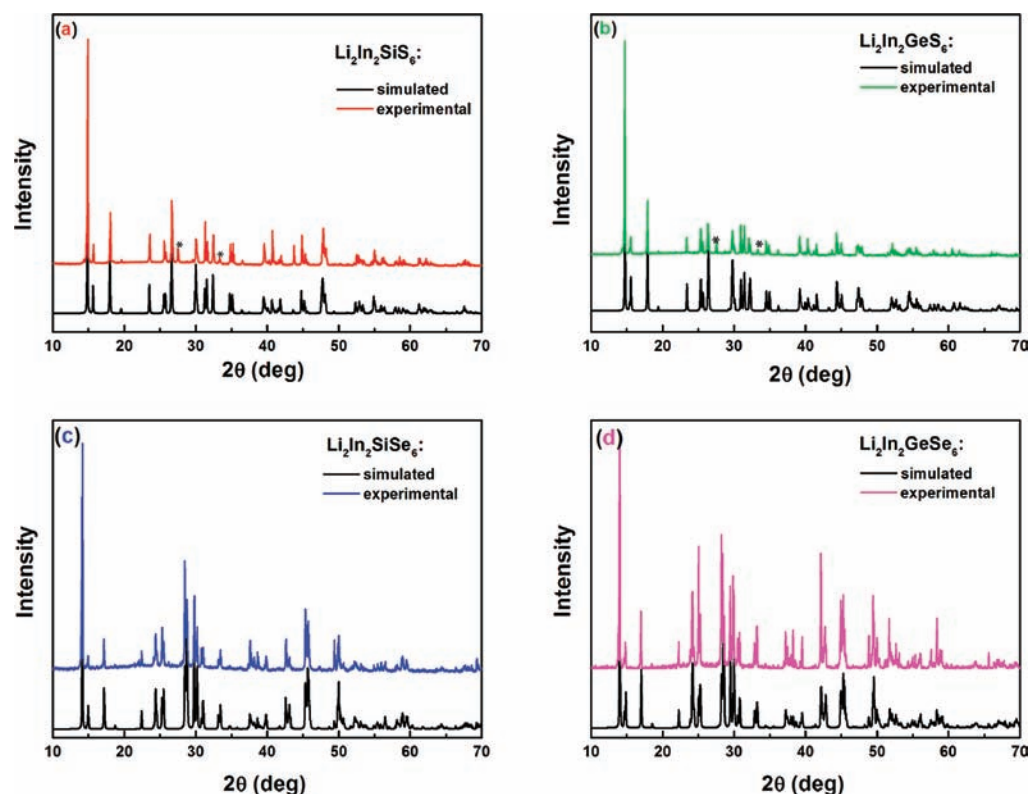


Figure 1. Powder XRD patterns of $\text{Li}_2\text{In}_2\text{MQ}_6$ ($M = \text{Si, Ge; Q} = \text{S, Se}$). The peaks marked with asterisks in $\text{Li}_2\text{In}_2\text{SiS}_6$ and $\text{Li}_2\text{In}_2\text{GeS}_6$ are due to very small amounts of In_2S_3 .

IR NLO materials with the desired optical and thermal properties, $\text{Li}_2\text{In}_2\text{MQ}_6$ ($M = \text{Si, Ge; Q} = \text{S, Se}$). Interestingly, these series of compounds possess different stoichiometries and structures from $\text{LiGaGe}_2\text{Se}_6$. The two sulfides possess similar NLO response as benchmark material AgGaS_2 and larger band gaps than AgGaS_2 , while the two selenides possess similar NLO response as benchmark material AgGaSe_2 and larger band gaps than AgGaSe_2 . Moreover, all the four compounds in this series exhibit congruent-melting behavior. In this paper, we report the synthesis, structure, and optical and thermal physical properties of the $\text{Li}_2\text{In}_2\text{MQ}_6$ ($M = \text{Si, Ge; Q} = \text{S, Se}$) compounds.

EXPERIMENTAL SECTION

Syntheses. Li was purchased from Alfa Aesar China (Tianjin) Co., Ltd., with a purity of 98%, while In, Si, Ge, S, and Se were purchased from Sinopharm Chemical Reagent Co., Ltd., with purities of 4 N. All of the above chemicals were used without further purification.

The binary starting materials Li_2Q ($\text{Q} = \text{S, Se}$) were prepared by the stoichiometric reactions of Li with Q (S, Se) in liquid NH_3 at 194 K, while In_2S_3 , In_2Se_3 , GeS_2 , GeSe_2 , SiS_2 , and SiSe_2 were synthesized by the stoichiometric reactions of elements at high temperatures in sealed silica tubes evacuated to 10^{-3} Pa. The ternary LiInQ_2 ($\text{Q} = \text{S, Se}$) were synthesized by the stoichiometric reactions of the binary chalcogenides at high temperatures in sealed silica tubes evacuated to 10^{-3} Pa.

During the crystal growth and synthesis of the polycrystalline samples of $\text{Li}_2\text{In}_2\text{MQ}_6$ ($M = \text{Si, Ge; Q} = \text{S, Se}$), all reactants were ground, loaded into 12-mm-i.d. fused-silica tubes under an Ar atmosphere in a glovebox, then moved to a high-vacuum line, and flame-sealed under a high vacuum of 10^{-3} Pa. The tubes were then placed in computer-controlled furnaces and heated according to the heating profiles detailed below.

$\text{Li}_2\text{In}_2\text{MS}_6$ ($M = \text{Si, Ge}$). The mixtures of LiInS_2 (1 mmol) and MS_2 ($M = \text{Si, Ge; 0.5 mmol}$) were heated to 1173 K in 15 h, left for 48 h, cooled to 593 K at a rate of 3 K/h, and finally cooled to room

temperature by switching off the furnace. Many block-shaped crystals with the color of light yellow were found in the ampules. The crystals are stable in air.

$\text{Li}_2\text{In}_2\text{MSe}_6$ ($M = \text{Si, Ge}$). The mixtures of LiInSe_2 (1 mmol) and MSe_2 ($M = \text{Si, Ge; 0.5 mmol}$) were heated to 1123 K in 12 h, left for 48 h, cooled to 473 K at a rate of 4 K/h, and finally cooled to room temperature by switching off the furnace. Many orange block-shaped crystals were found in the ampules. The crystals are stable in air.

The block-shaped crystals were manually selected for structure characterization and determined as $\text{Li}_2\text{In}_2\text{MQ}_6$ ($M = \text{Si, Ge; Q} = \text{S, Se}$). Analyses of the crystals with an energy-dispersive-X-ray (EDX)-equipped Hitachi S-4800 scanning electron microscope showed the presence of In, M (Si, Ge), and Q (S, Se) in the approximate ratio of 2:1:6 (Li is undetectable in EDX).

Polycrystalline samples of $\text{Li}_2\text{In}_2\text{MQ}_6$ ($M = \text{Si, Ge; Q} = \text{S, Se}$) were synthesized by solid-state reaction techniques. The mixtures of Li_2Q , MQ_2 , and In_2Q_3 ($M = \text{Si, Ge; Q} = \text{S, Se}$) in the molar ratio of 1:1:1 were heated to 973 K in 15 h and kept at that temperature for 72 h, and then the furnace was turned off.

Powder X-ray diffraction (XRD) analyses of the resultant powder samples were performed at room temperature in the angular range of $2\theta = 10\text{--}70^\circ$ with a scan step width of 0.02° and a fixed counting time of 0.1 s/step using an automated Bruker D8 X-ray diffractometer equipped with a diffracted monochromator set for $\text{Cu K}\alpha$ ($\lambda = 1.5418 \text{ \AA}$) radiation. The experimental powder XRD patterns were found to be in agreement with the calculated pattern on the basis of the single-crystal crystallographic data of $\text{Li}_2\text{In}_2\text{MQ}_6$ ($M = \text{Si, Ge; Q} = \text{S, Se}$; Figure 1).

Structure Determination. The single-crystal XRD measurements were performed on a Bruker SMART APEX II diffractometer at 296(2) K using $\text{Mo K}\alpha$ radiation ($\lambda = 0.71073 \text{ \AA}$) and integrated with the SAINT program.²⁰ The program XPREP²¹ was used for face-indexed absorption corrections.

The structure was solved with direct methods implemented in the program SHELXS and refined with the least-squares program SHELXL of the SHELXTL PC suite of programs.²¹ The program STRUCTURE

TIDY²² was then employed to standardize the atomic coordinates. Additional experimental details are given in Table 1, and selected metrical data are given in Table 2. Further information can be found in the Supporting Information.

Table 1. Crystal Data and Structure Refinements for $\text{Li}_2\text{In}_2\text{MQ}_6$ (M = Si, Ge; Q = S, Se)

	$\text{Li}_2\text{In}_2\text{SiS}_6$	$\text{Li}_2\text{In}_2\text{GeS}_6$	$\text{Li}_2\text{In}_2\text{SiSe}_6$	$\text{Li}_2\text{In}_2\text{GeSe}_6$
fw	463.97	508.47	745.37	789.87
T (°C)	23	23	23	23
a (Å)	12.0741(11)	12.165(2)	12.6210(4)	12.7226(4)
b (Å)	7.0221(5)	7.0840(14)	7.3788(3)	7.4527(4)
c (Å)	12.0802(9)	12.131(2)	12.5800(4)	12.6698(5)
β (deg)	110.060(5)	110.26(3)	109.704(2)	109.826(4)
V (Å ³)	962.09(13)	980.7(3)	1102.95(7)	1130.12(8)
space group	Cc	Cc	Cc	Cc
Z	4	4	4	4
ρ_c (g/cm ³)	3.203	3.444	4.489	4.642
μ (cm ⁻¹)	6.139	8.906	24.021	25.946
$R(F)^a$	0.0098	0.0215	0.0221	0.0338
$R_w(F_o^2)^b$	0.0231	0.0501	0.0534	0.0791

^a $R(F) = \sum ||F_o| - |F_c|| / \sum |F_o|$ for $F_o^2 > 2\sigma(F_o^2)$. ^b $R_w(F_o^2) = \{ \sum [w(F_o^2 - F_c^2)^2] / \sum wF_o^4 \}^{1/2}$ for all data. $w^{-1} = \sigma^2(F_o^2) + (zP)^2$, where $P = (\max(F_o^2, 0) + 2F_c^2) / 3$; $z = 0.01$ for $\text{Li}_2\text{In}_2\text{SiS}_6$ and 0.04 for the other three.

Table 2. Selected Interatomic Distances (Å) for $\text{Li}_2\text{In}_2\text{MQ}_6$ (M = Si, Ge; Q = S, Se)

	$\text{Li}_2\text{In}_2\text{SiS}_6$	$\text{Li}_2\text{In}_2\text{GeS}_6$	$\text{Li}_2\text{In}_2\text{SiSe}_6$	$\text{Li}_2\text{In}_2\text{GeSe}_6$
Li1–Q1	2.510(4)	2.522(9)	2.64(1)	2.66(2)
Li1–Q2	2.493(4)	2.549(9)	2.61(1)	2.64(2)
Li1–Q4	2.716(6)	2.66(1)	2.86(2)	2.86(3)
Li1–Q5	2.513(4)	2.522(9)	2.64(1)	2.69(2)
Li2–Q1	2.494(4)	2.523(9)	2.63(1)	2.66(2)
Li2–Q2	2.508(5)	2.544(9)	2.64(1)	2.65(2)
Li2–Q3	2.518(5)	2.520(9)	2.62(1)	2.69(2)
Li2–Q6	2.566(5)	2.548(9)	2.66(1)	2.65(3)
In1–Q1	2.4564(5)	2.459(1)	2.5776(8)	2.584(1)
In1–Q2	2.4630(6)	2.468(1)	2.5843(7)	2.592(1)
In1–Q3	2.5032(5)	2.498(1)	2.6194(7)	2.614(1)
In1–Q5	2.4750(5)	2.471(1)	2.6014(7)	2.599(1)
In2–Q1	2.4685(5)	2.466(1)	2.5892(8)	2.591(1)
In2–Q2	2.4733(5)	2.480(1)	2.5931(8)	2.597(1)
In2–Q4	2.4918(6)	2.488(2)	2.6097(7)	2.612(1)
In2–Q6	2.4708(5)	2.467(1)	2.5931(7)	2.594(1)
M–Q3	2.1072(7)	2.1801(1)	2.251(2)	2.323(1)
M–Q4	2.1040(7)	2.184(1)	2.239(2)	2.314(1)
M–Q5	2.1199(7)	2.197(1)	2.257(2)	2.331(1)
M–Q6	2.1166(7)	2.188(1)	2.255(2)	2.323(1)

Diffuse-Reflectance Spectroscopy. A Cary 1E UV–visible spectrophotometer with a diffuse-reflectance accessory was used to measure the spectra of $\text{Li}_2\text{In}_2\text{MQ}_6$ (M = Si, Ge; Q = S, Se) over the range 200 nm (6.2 eV) to 1800 nm (0.69 eV).

Thermal Analysis. The thermal properties were investigated by differential scanning calorimetry (DSC) analysis using a Labsys TG-DTA16 (SETARAM) thermal analyzer (the calorimeter was calibrated with Al_2O_3). About 10 mg of each $\text{Li}_2\text{In}_2\text{MQ}_6$ (M = Si, Ge; Q = S, Se) sample was placed in sealed carbon-coated silica tubes evacuated to 10^{-3} Pa. The heating and cooling rates were 20 K/min.

SHG Measurement. Optical SHG tests of $\text{Li}_2\text{In}_2\text{MQ}_6$ (M = Si, Ge; Q = S, Se) were performed on the powder samples by means of the Kurtz–Perry method.²³ Fundamental 2090 nm light was generated

with a Q-switched Ho:Tm:Cr:YAG laser. The particle sizes of the sieved samples are 80–100 μm . Microcrystalline AgGaS_2 and AgGaSe_2 of similar particle size served as references for the two sulfides and two selenides, respectively.

RESULTS AND DISCUSSION

Structure. The four compounds $\text{Li}_2\text{In}_2\text{MQ}_6$ (M = Si, Ge; Q = S, Se) are isostructural. They belong to the Cd_4GeS_6 structure type²⁴ and crystallize in the noncentrosymmetric space group Cc of the monoclinic system. In the asymmetric unit, there are two crystallographically independent Li atoms, two independent In atoms, one M (Si, Ge) atom, and six Q (S, Se) atoms. All of the atoms are at general positions with 100% occupancy, and there is no detectable disorder among Li, In, or M (Si, Ge) atoms in the structure, although the possibility of such disorder cannot be completely ruled out. Because there are no Q–Q (Q = S, Se) bonds in the structures, the oxidation states of 1+, 3+, 4+, and 2– can be assigned to Li, In, M (Si, Ge), and Q (S, Se), respectively.

The structure of $\text{Li}_2\text{In}_2\text{SiS}_6$ is illustrated in Figure 2. The LiS_4 , InS_4 , and SiS_4 tetrahedra are connected to each other via

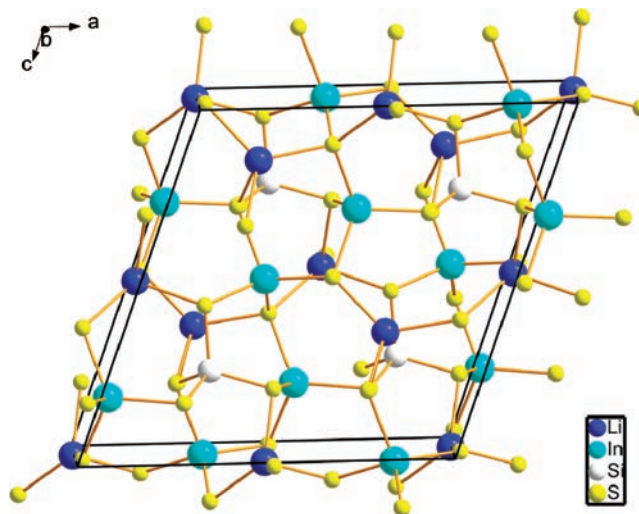


Figure 2. Unit cell of the $\text{Li}_2\text{In}_2\text{SiS}_6$ structure.

corner-sharing to generate a three-dimensional framework. In comparison, another compound in the quaternary Li/M/M'/Q (M = Si, Ge; M' = Al, Ga, In; Q = S, Se, Te) system, namely, $\text{LiGaGe}_2\text{Se}_6$, has some differences with $\text{Li}_2\text{In}_2\text{MQ}_6$ (M = Si, Ge; Q = S, Se) in the structure. $\text{LiGaGe}_2\text{Se}_6$ crystallizes in the orthorhombic space group $Fdd2$ with the asymmetric unit containing one crystallographically independent Li atom at the Wyckoff position 16b with 50% occupancy, one independent Ga atom at the Wyckoff position 8a, one independent Ge atom at the Wyckoff position 16b, and three independent Se atoms at the Wyckoff position 16b, leading to $\text{LiGaGe}_2\text{Se}_6$ stoichiometry. $\text{LiGaGe}_2\text{Se}_6$ also has a three-dimensional framework built up from corner-sharing LiSe_4 , GaSe_4 , and GeSe_4 tetrahedra, but the Li position is only half-occupied in $\text{LiGaGe}_2\text{Se}_6$.

Selected bond distances are listed in Table 2. For the two sulfides, the Li–S distances range from 2.493(4) to 2.716(6) Å, which are close to those in LiInS_2 (2.392–2.750 Å);²⁵ the In–S distances of 2.4564(5)–2.5032(5) Å are comparable to the In–S distances of 2.392–2.500 Å in $\text{Ba}_2\text{In}_2\text{S}_5$;²⁶ the Si–S distances of 2.1040(7)–2.1199(7) Å are close to those in KBiSi_4 [2.094(1)–2.155(2) Å];²⁷ the Ge–S distances of

2.1801(1)–2.197(1) Å are comparable to those of 2.180(2)–2.239(2) Å in KBiGeS_4 ²⁷ and 2.208(1)–2.265(1) Å in AgGaGeS_4 .²⁸ As for the two selenides, the Li–Se distances of 2.61(1)–2.86(3) Å are in good agreement with those of 2.64(3)–2.83(3) Å in $\text{LiGaGe}_2\text{Se}_6$,⁵ the In–Se distances range from 2.5776(8) to 2.6194(7) Å, which resemble those of 2.569 Å in LiInSe_2 ,²⁹ the Si–Se distances of 2.239(2)–2.257(2) Å are comparable to those of 2.224–2.328 Å in $\text{Ag}_2\text{In}_2\text{SiSe}_6$,³⁰ the Ge–Se distances range from 2.314(1) to 2.331(1) Å, which are in good agreement with those in $\text{Ag}_2\text{In}_2\text{GeSe}_6$ (2.313–2.336 Å).³¹

Experimental Band Gaps. On the basis of the UV–visible–near-IR diffuse-reflectance spectra of $\text{Li}_2\text{In}_2\text{MQ}_6$ (M = Si, Ge; Q = S, Se; Figure 3), the band gaps are 3.61(2), 3.45(2),

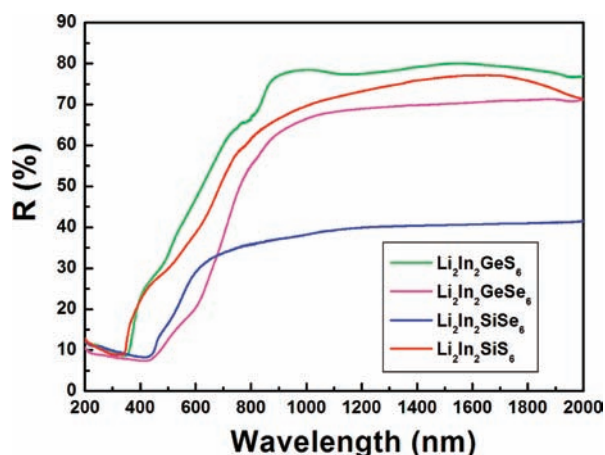


Figure 3. Diffuse-reflectance spectra of $\text{Li}_2\text{In}_2\text{MQ}_6$ (M = Si, Ge; Q = S, Se).

2.54(2), and 2.30(2) eV, and consequently the absorption edges are 343, 360, 490, and 540 nm for $\text{Li}_2\text{In}_2\text{SiS}_6$, $\text{Li}_2\text{In}_2\text{GeS}_6$, $\text{Li}_2\text{In}_2\text{SiSe}_6$, and $\text{Li}_2\text{In}_2\text{GeSe}_6$, respectively, as deduced by a straightforward extrapolation method.³² The band gaps of the two sulfides are significantly larger than that of AgGaS_2 (2.64 eV), while those of the two selenides are also obviously larger than that of AgGaSe_2 (1.8 eV). Owing to this large band gap, the $\text{Li}_2\text{In}_2\text{MQ}_6$ (M = Si, Ge; Q = S, Se) compounds may possess high laser-induced damage thresholds. Moreover, the pumping sources can be conventional near-IR laser pumping (Nd:YAG or Yb:YAG) or even the 800 nm Ti:sapphire laser without two-photon absorption problems, as in the case of LiInS_2 .³³

Thermal Analysis. The DSC curves of $\text{Li}_2\text{In}_2\text{MQ}_6$ (M = Si, Ge; Q = S, Se) are shown in Figure 4. It shows that $\text{Li}_2\text{In}_2\text{MQ}_6$ (M = Si, Ge; Q = S, Se) compounds melt congruently, with the melting points being 858 °C, 780 °C, 801 °C, and 722 °C for $\text{Li}_2\text{In}_2\text{SiS}_6$, $\text{Li}_2\text{In}_2\text{GeS}_6$, $\text{Li}_2\text{In}_2\text{SiSe}_6$, and $\text{Li}_2\text{In}_2\text{GeSe}_6$, respectively. Owing to the congruent-melting behavior, bulk crystals needed for thorough evaluation and practical application can be grown by the Bridgman–Stockbarger technique. These melting points are lower than those of traditional IR NLO materials (1025 °C for ZnGeP_2 , 998 °C for AgGaS_2 , and 860 °C for AgGaSe_2). The rather low melting points of $\text{Li}_2\text{In}_2\text{MQ}_6$ (M = Si, Ge; Q = S, Se) will favor crystal growth by the Bridgman–Stockbarger technique.

SHG Measurement. With the use of a laser with 2090 nm as the fundamental wavelength and with similar particle size, the SHG signal intensities of the two sulfides were close to that of AgGaS_2 and those for the two selenides were similar to that of AgGaSe_2 , which indicate that the NLO responses of $\text{Li}_2\text{In}_2\text{MQ}_6$ (M = Si, Ge; Q = S, Se) compounds are sufficient for application in IR nonlinear optics.

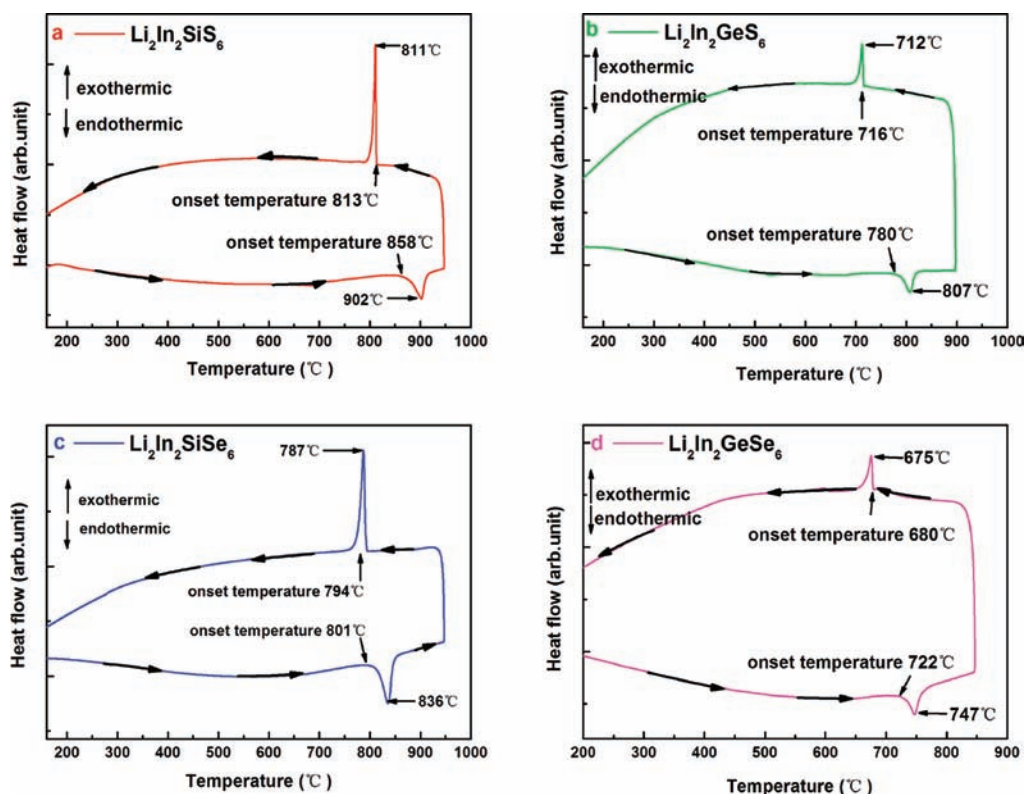


Figure 4. DSC curves of $\text{Li}_2\text{In}_2\text{MQ}_6$ (M = Si, Ge; Q = S, Se).

CONCLUSION

A new series of IR NLO material $\text{Li}_2\text{In}_2\text{MQ}_6$ ($M = \text{Si, Ge; Q} = \text{S, Se}$) have been synthesized for the first time. They adopt the Cd_4GeS_6 structure type and crystallize in the noncentrosymmetric space group Cc . The LiQ_4 , InQ_4 , and MQ_4 ($M = \text{Si, Ge; Q} = \text{S, Se}$) tetrahedra are connected to each other by corner-sharing to generate a three-dimensional framework. $\text{Li}_2\text{In}_2\text{MQ}_6$ ($M = \text{Si, Ge; Q} = \text{S, Se}$) exhibit SHG responses at $2 \mu\text{m}$ that are approximately close to those of benchmark AgGaQ_2 ($Q = \text{S, Se}$). Their large band gaps will be very beneficial to increase the laser-damage threshold and avoid the two-photon absorption of the conventional $1 \mu\text{m}$ (Nd:YAG) or $1.55 \mu\text{m}$ (Yb:YAG) laser pumping. Moreover, the valuable property of congruent-melting behavior for all of the four compounds makes it feasible to grow bulk crystals needed for thorough evaluation and practical application by the Bridgman–Stockbarger method. Our preliminary experimental results indicated that $\text{Li}_2\text{In}_2\text{MQ}_6$ are promising IR NLO materials for practical application. Further research is in progress.

ASSOCIATED CONTENT

Supporting Information

Crystallographic file in CIF format for $\text{Li}_2\text{In}_2\text{MQ}_6$ ($M = \text{Si, Ge; Q} = \text{S, Se}$). This material is available free of charge via the Internet at <http://pubs.acs.org>.

AUTHOR INFORMATION

Corresponding Author

*E-mail: jyao@mail.ipc.ac.cn.

Notes

The authors declare no competing financial interest.

ACKNOWLEDGMENTS

This research was supported by the National Basic Research Project of China (Grant 2010CB630701), National Natural Science Foundation of China (Grant 51072203), and the Scientific Research Foundation for the Returned Overseas Chinese Scholars, State Education Ministry.

REFERENCES

- (1) Chemla, D. S.; Kupecek, P. J.; Robertson, D. S.; Smith, R. C. *Opt. Commun.* **1971**, *3*, 29–31.
- (2) Boyd, G. D.; Kasper, H. M.; McFee, J. H.; Storz, F. G. *IEEE J. Quantum Electron.* **1972**, *8*, 900–908.
- (3) Boyd, G. D.; Buehler, E.; Storz, F. G. *Appl. Phys. Lett.* **1971**, *18*, 301–304.
- (4) Schunemann, P. G. *AIP Conf. Proc.* **2007**, *916*, 541–559.
- (5) Mei, D.; Yin, W.; Feng, K.; Lin, Z.; Bai, L.; Yao, J.; Wu, Y. *Inorg. Chem.* **2012**, *51*, 1035–1040.
- (6) Bera, T. K.; Song, J. H.; Freeman, A. J.; Jang, J. I.; Ketterson, J. B.; Kanatzidis, M. G. *Angew. Chem., Int. Ed.* **2008**, *47*, 7828–7832.
- (7) Isaenko, L.; Vasilyeva, I.; Merkulov, A.; Yelissev, A.; Lobanov, S. *J. Cryst. Growth* **2005**, *275*, 217–223.
- (8) Lin, X.; Zhang, G.; Ye, N. *Cryst. Growth Des.* **2009**, *9*, 1186–1189.
- (9) Yao, J.; Mei, D.; Bai, L.; Lin, Z.; Yin, W.; Fu, P.; Wu, Y. *Inorg. Chem.* **2010**, *49*, 9212–9216.
- (10) Mei, D.; Yin, W.; Bai, L.; Lin, Z.; Yao, J.; Fu, P.; Wu, Y. *Dalton Trans.* **2011**, *40*, 3610–3615.
- (11) Kim, Y.; Seo, I. S.; Martin, S. W.; Baek, J.; Halasyamani, P. S.; Arumugam, N.; Steinfink, H. *Chem. Mater.* **2008**, *20*, 6048–6052.
- (12) Geng, L.; Cheng, W.-D.; Lin, C.-S.; Zhang, W.-L.; Zhang, H.; He, Z.-Z. *Inorg. Chem.* **2011**, *50*, 5679–5686.
- (13) Chen, M.-C.; Li, L.-H.; Chen, Y.-B.; Chen, L. *J. Am. Chem. Soc.* **2011**, *133*, 4617–4624.
- (14) Liao, J.-H.; Marking, G. M.; Hsu, K. F.; Matsushita, Y.; Ewbank, M. D.; Borwick, R.; Cunningham, P.; Rosker, M. J.; Kanatzidis, M. G. *J. Am. Chem. Soc.* **2003**, *125*, 9484–9493.
- (15) Guo, S. P.; Guo, G. C.; Wang, M. S.; Zou, J. P.; Xu, G.; Wang, G. J.; Long, X. F.; Huang, J. S. *Inorg. Chem.* **2009**, *48*, 7059–7065.
- (16) Banerjee, S.; Malliakas, C. D.; Jang, J. I.; Ketterson, J. B.; Kanatzidis, M. G. *J. Am. Chem. Soc.* **2008**, *130*, 12270–12272.
- (17) Chung, I.; Song, J. H.; Jang, J. I.; Freeman, A. J.; Ketterson, J. B.; Kanatzidis, M. G. *J. Am. Chem. Soc.* **2009**, *131*, 2647–2656.
- (18) Bai, L.; Lin, Z.; Wang, Z.; Chen, C.; Lee, M. H. *J. Chem. Phys.* **2004**, *120*, 8772–8778.
- (19) Bai, L.; Lin, Z.; Wang, Z.; Chen, C. *J. Appl. Phys.* **2008**, *103*, 083111/1–083111/6.
- (20) SAINT, version 7.60A; Bruker Analytical X-ray Instruments, Inc.: Madison, WI, 2008.
- (21) Sheldrick, G. M. *Acta Crystallogr., Sect. A* **2008**, *64*, 112–122.
- (22) Gelato, L. M.; Parthé, E. *J. Appl. Crystallogr.* **1987**, *20*, 139–143.
- (23) Kurtz, S. K.; Perry, T. T. *J. Appl. Phys.* **1968**, *39*, 3798–3813.
- (24) Julien-Pouzol, M.; Jaulmes, S. *Acta Crystallogr., Sect. C* **1995**, *51*, 1966–1968.
- (25) Kish, Z. Z.; Kanishcheva, A. S.; Mikhailov, Yu. N.; Lazarev, V. B.; Semrad, E. E.; Peresh, E. Yu. *Dokl. Akad. Nauk SSSR* **1985**, *280*, 398–401.
- (26) Eisenmann, B.; Hofmann, A. *Z. Anorg. Allg. Chem.* **1990**, *580*, 151–159.
- (27) Mei, D.; Lin, Z.; Bai, L.; Yao, J.; Fu, P.; Wu, Y. *J. Solid State Chem.* **2010**, *183*, 1640–1644.
- (28) Pobedimskaja, E. A.; Alimova, L. L.; Belov, N. V.; Badikov, V. V. *Dokl. Akad. Nauk SSSR* **1981**, *257*, 611–614.
- (29) Beister, H. J.; Ves, S.; Hönle, W.; Syassen, K.; Kühn, G. *Phys. Rev. B* **1991**, *43*, 9635–9642.
- (30) Olekseyuk, I. D.; Sachanyuk, V. P.; Parasyuk, O. V. *J. Alloys Compd.* **2006**, *414*, 73–77.
- (31) Krykhovets, O. V.; Sysa, L. V.; Olekseyuk, I. D.; Glowyak, T. J. *J. Alloys Compd.* **1999**, *287*, 181–184.
- (32) Schevciw, O.; White, W. B. *Mater. Res. Bull.* **1983**, *18*, 1059–1068.
- (33) Rotermund, F.; Petrov, V.; Noack, F.; Isaenko, L.; Yelissev, A.; Lobanov, S. *Appl. Phys. Lett.* **2001**, *78*, 2623–2625.